Lattice Thermal Conductivity and Deviations from Matthiessen's Rule for Dilute Alloys of Tin with Cadmium*

M. C. Karamargin,† C. A. Reynolds,‡ F. P. Lipschultz, and P. G. Klemens
Department of Physics and Institute of Materials Science, University of Connecticut, Storrs, Connecticut 06268
(Received 26 May 1972)

The thermal and electrical conductivities of six single crystals of tin with cadmium (cadmium content ranging from 0.24 to 0.97 at.%) have been measured from 4.2 to about 80 K. The lattice thermal conductivity was deduced for three of these samples of cadmium content in excess of 0.70 at.%, oriented close to 78° with respect to the tetragonal axis. Values of the ideal thermal resistivity of pure tin were needed to effect the separation into lattice and electronic components at higher temperatures, and it was assumed that deviations from Matthiessen's rule for thermal resistivity were governed by measured electrical-resistivity deviations and the Wiedemann–Franz law. The lattice thermal conductivity was analyzed in terms of phonon scattering by electrons, point defects, and anharmonic phonon interactions. Below 12 K the three samples gave a lattice thermal conductivity proportional to T^2 and of magnitude $1.5\times10^{-4}\,T^2$ W cm^{-1} K^{-1}, rising to a maximum of about 0.045 W cm^{-1} K^{-1} near 40 K. Deviations from Matthiessen's rule for the electrical resistivity were obtained for all six samples. These deviations show a T^2 dependence at low temperatures. This is inconsistent with a two-band model but suggests phonon-assisted impurity scattering. A theoretical difficulty associated with this mechanism is discussed.

I. INTRODUCTION

Previous experimental investigations of the thermal conductivity of tin alloys gave information on the lattice thermal conductivity in the superconducting state, and made it desirable to determine the lattice component in the normal state above 4.2 K. There is a surprising lack of electrical- and thermal-conductivity data from 4.2 to 77 K. The present measurements were made to determine the lattice component, but in order to separate the lattice and electronic components with some confidence, it was found necessary to measure the thermal conductivity of pure tin in that temperature range, and to study the deviations from Matthiessen's rule of the electrical resistivity. The measurements on pure tin have been reported previously[1]; the present paper reports the measurements on six single crystals of dilute alloys of cadmium in tin. All samples have their axis oriented nearly perpendicular to the tetragonal axis. The cadmium content varies from 0.24 to 0.97 at.%. Only three samples, those with most cadmium, could be used to deduce an adequate measure of the lattice thermal conductivity, which agreed roughly with theoretical expectations. All the samples provided information on the dependence of the deviations from Matthiessen's rule with temperature and solute content.

II. EXPERIMENTAL METHOD

A. Sample Preparation

All the samples used in the experiment were prepared from Johnson–Matthey spectroscopically pure 99.999% tin and 99.999% cadmium obtained from the Jarrell–Ash Co., Waltham, Mass. They were single crystals grown by the Bridgeman technique[2] in precision-bore glass tubing, either 2- or 3-mm i.d. The samples are summarized in Table I. Samples 6–8, 3 mm in diameter, are the identical samples grown and reported by Gueths *et al.*,[3] who designated them as Nos. 5–7. Samples 3–5, having the lowest cadmium content, are of 2-mm diameter, prepared by a method described previously.[1] Also listed is the angle between the sample axis and the tetragonal axis of the crystal, as determined by an optical goniometer.[4] The values of ρ_0 are the residual resistivities, measured at 4.2 K. The solute content given is deduced from the residual resistivity, using the linear relation $\rho_0 = 1.39\times10^{-6}\ \Omega$ cm (at.%)$^{-1}$, taken from Gueths *et al.*[5] for perpendicularly oriented samples. The values of ρ_0 in the case of samples 6–8 are values obtained in the present work; they are nearly iden-

TABLE I. Resumé of all measured samples. The constant of proportionality b was determined by a computer fit to the measured deviations from Matthiessen's rule ($\Delta\rho_i$) according to the relation $\Delta\rho_i = b\ \rho_0 T^2$.

Sample No.	Cd impurity (at.%)	Sample axis relative to crystal c axis (deg)	ρ_0 ($\mu\Omega$ cm)	b (K^{-2})
3	0.24	86	0.330	5.25×10^{-5}
4	0.41	90	0.560	5.25×10^{-5}
5	0.57	83	0.782	5.89×10^{-5}
6	0.74	79	1.020	12.02×10^{-5}
7	0.90	78	1.206	3.38×10^{-5}
8	0.97	77	1.346	6.46×10^{-5}

tical to the values previously reported. All the samples are single crystals 5–7 cm in length. All samples were sealed in vacuum and annealed at approximately 180 °C for 350 h prior to the low-temperature measurements. The accuracy of the optical orientation is felt to be within 1.5°.

B. Cryostat and Measurement

The variable-temperature cryostat that was utilized for this experiment is the same one used in measuring the pure-tin samples reported in a previous paper.[1] It consists basically of a thermally isolated platform and heat exchanger that is mounted inside a vacuum chamber. The chamber itself is large enough so that four samples can be measured at the same time. This fact minimizes the waiting period that is required for thermal equilibrium at the higher temperatures. The vacuum chamber of the variable-temperature cryostat is surrounded with liquid helium after each transfer and the thermal platform inside the chamber is cooled by a steady flow of helium vapor. The samples are suspended in vacuum from the thermal platform with thermal-conductivity measurements being made by measuring the thermal gradients that are applied along each sample's length. Temperature control is provided by means of a standard regulating circuit that controls the current to a heater that is wound over the heat exchanger.

All temperatures were determined by monitoring the electrical resistance of Cryocal, Inc., germanium resistors that were calibrated according to the manufacturer's specifications. Each resistor was attached to small copper clips that also served as potential probes for the determination of electrical resistivity. Once placed on a sample, these clips were not disturbed until all thermal- and electrical-conductivity measurements were completed. This eliminated any geometrical error associated with relating the two different sets of data. On each sample, however, separate experimental runs were required for either a thermal- or electrical-conductivity measurement. The experimental procedure by which all thermal- and electrical-conductivity measurements were made was identical to that described in the earlier work[1] with the probable errors associated with the present measurements being identical in most respects to those mentioned there. However, in the case of alloys, the low-temperature electrical-resistivity values are now much higher and therefore easier to measure. The probable error associated with any low-temperature electrical-resistivity measurement was found to be never more than 0.5% below 20 K or 0.6% above 35 K. These limits were obtained with resistivity currents up to $\frac{1}{3}$ A, which were small enough as not to cause any measurable heating of the sample over short periods of time. As an extra precaution against the occurrence of this effect, the resistance of the germanium sensors attached to the copper clips on each sample were continuously monitored in order to be certain that no measurable temperature gradient was present during a resistivity measurement.

All thermal-conductivity measurements were corrected for stray heat losses resulting from the wiring connections on the warm end of the sample. A small correction for the heat generated in the leads carrying current to the sample heaters was also made. The heaters themselves consist of small copper spools over which 70 ft of 0.0025-in. Evanohm wire is wound noninductively. This wire provides a resistance on the order of 9000 Ω that was found to be constant to within 0.1% at all temperatures from 4.2 to 75 K. Heat losses due to radiation were minimized by enclosing all of the samples inside a copper-foil radiation shield that was held at the temperature of the thermal platform. Only when temperature differences greater than 3 K were applied to the sample, usually at temperatures somewhere above 60 K, was it found necessary to employ a small radiation correction. At worst, this correction never exceeded 1% of the heater power. The probable error in the thermal conductivity results essentially from a fixed error in the geometrical factor and a calibration error associated with the uncertainty in the true temperature. The latter increases with temperature, as specified by Cryocal, Inc., and results in a total probable error order of 1% at temperatures above 40 K. At lower temperatures the probable error gets smaller, being close to 0.5% below 20 K.

III. EXPERIMENTAL RESULTS

A. Thermal Conductivity

The total thermal conductivity was determined by the longitudinal heat flow, and the thermal conductivity K is given by $K = QL/(A\,\Delta T)$, where Q is the steady heat flow, A is the cross-sectional area, L is the distance between the points of thermometer attachment, and ΔT is the temperature difference between them. These measured values of K are shown by the solid curves of Fig. 1 for the six alloy samples. The thermal conductivities of two pure-tin crystals, P-1 and P-3, reported earlier,[1] are also shown. These samples are oriented nearly parallel (6°) and perpendicular (72°) with respect to the tetragonal axis.

In general, the behavior of all six alloyed samples is as expected; the conductivity decreases with increasing solute content. Since all of these samples have nearly perpendicular crystallographic

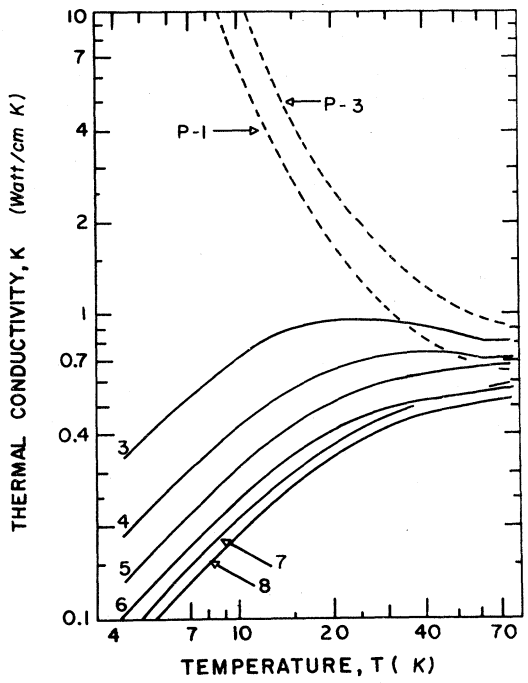

FIG. 1. Total measured thermal conductivity of all six alloy samples and the two pure samples.

orientation they will all fall below the pure (72°) sample P-3. As can be seen from the curves, samples 3–5 all exceed the parallel sample P-1 in conductivity above 60 K. The only anomalous behavior in the total thermal conductivity appears in the measured values of sample 6 above 20 K. Here, the total thermal conductivity dips down below the values obtained for sample 7, a sample with more cadmium present. Samples 7 and 8 both show very similar behavior, with their conductivities approximately parallel over the entire temperature range. We believe that the solute content in sample 6 may be inhomogeneously distributed. The two most dilute alloy samples (3 and 4) show broad maxima in their thermal conductivity at approximately 25 and 40 K, respectively; the maximum of sample 4 is less pronounced.

B. Electrical Resistivity

The results of the electrical-resistivity measurements made on the six samples by the potentiometric technique can be seen in Fig. 2. Again, the measured values for the two pure samples P-1 and P-3 are shown by the two dashed lines for comparison. The electrical resistivity behaves as expected with the samples of highest solute content showing a dominance of the residual resistivity ρ_0 up to 10 K. At higher temperatures, the additive effect of the ideal resistivity ρ_i causes the total resistance to increase, with the family of lines converging on a logarithmic scale. As in the thermal conductivity, the resistivity of sample 6 is again anomalous, crossing the curve of sample 7 at approximately 50 K.

Most of the measured resistivity curves could be represented by the relation

$$\rho = \rho_0 + \beta\left(\frac{T}{\Theta}\right)^5 \int_0^{\Theta/T} \frac{x^5 e^x\, dx}{(e^x - 1)^2} \ , \tag{1}$$

where the term ρ_0 is the residual resistivity, as given by $\rho_{4.2}$ in Table I. An adequate fit of all the experimental data was obtained by taking $\beta = 11.54 \times 10^{-6}\ \Omega$ cm and setting $\Theta = 125$ K.

Thus one can regard the electrical resistivity as additively composed of a residual resistivity ρ_0 and an ideal resistivity $\rho_i(T)$, the latter being independent of ρ_0. This additivity is Matthiessen's rule. It follows from theory if certain simplifying assumptions are made. The form of $\rho_i(T)$ chosen here is also based on a simplified model. In actual fact one would expect $\rho_i(T)$ to depart from the Bloch–Grüneisen form chosen above, and one would also expect $\rho_i(T)$ not to be independent of ρ_0. The latter departure, or deviation from Matthiessen's rule, can be expressed in terms of the following expression for the total resistivity:

$$\rho(T) = \rho_0 + \rho_i(T) + \Delta\rho_i \ , \tag{2}$$

where $\Delta\rho_i$ is a function of ρ_0 and T, and by definition vanishes if $\rho_0 = 0$ or if $T = 0$.

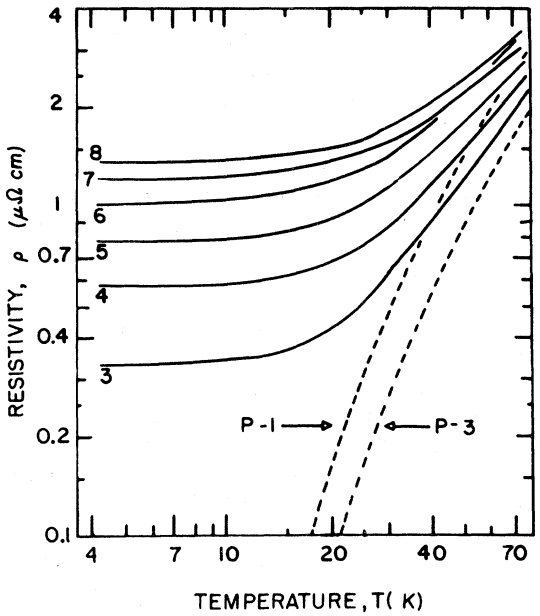

FIG. 2. Electrical resistivity of all six alloy samples and the two pure samples.

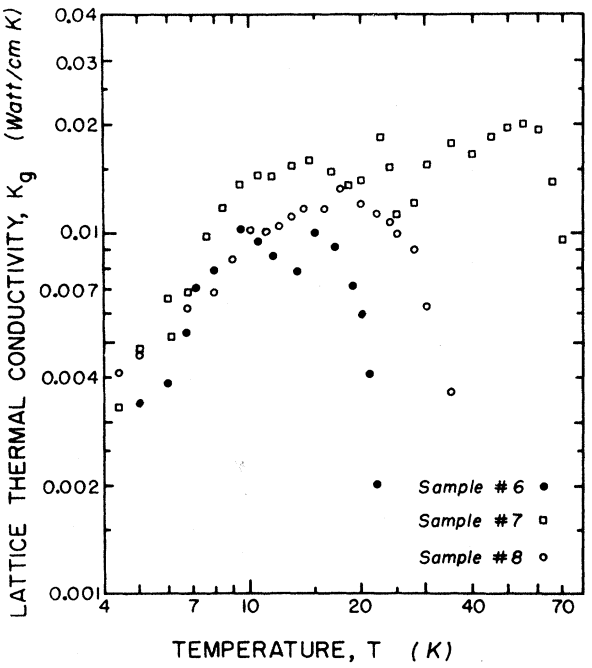

FIG. 3. Lattice thermal conductivity derived from Eq. (4).

IV. LATTICE THERMAL CONDUCTIVITY

A. Experimental Determination

The total thermal conductivity K of any alloy specimen can be given by

$$K = K_e + K_g \,, \tag{3}$$

where K_e is the electronic component and K_g is the lattice component. The electronic part K_e can be regarded as the reciprocal of the sum of the residual and intrinsic thermal resistivities W_0 and W_i. The lattice component K_g can then be obtained from

$$K_g = K - 1/(W_0 + W_i) \,. \tag{4}$$

The thermal and electrical residual resistivities W_0 and ρ_0 are related by the Wiedemann–Franz law

$$W_0 = \rho_0 / LT \,, \tag{5}$$

where T is the temperature and L is the Lorenz constant.

The essential difficulty that always arises with this type of analysis is the determination of the intrinsic resistivity W_i. It has sometimes been approximated by W_i deduced from thermal-conductivity measurements on pure samples.[6] This essentially neglects the contribution of the lattice component in a pure sample by assuming all of the conduction to be electronic. In this case, the intrinsic resistivity W_i is obtained from the thermal conductivity K_p and the residual resistivity ρ_{0p} of a reasonably pure metal by

$$W_i = (1/K_p) - \rho_{0p}/LT \,. \tag{6}$$

In view of the anisotropic transport properties of tin, one must take care to determine K_g by employing measurements of both pure and alloyed samples of nearly identical crystallographic orientations. The values of K_p and ρ_{0p} from sample P-3 were thus used in evaluating K_g from the alloy samples 6–8. The other three samples did not contain sufficient cadmium to allow for an adequate separation of the lattice term. The criterion for the lattice component to be separable is a sufficiently high residual resistivity, as first discussed by Kemp *et al.*[7,8]

The values of the lattice thermal conductivity thus obtained for these three samples are shown in Fig. 3. Except for a characteristic T^2 dependence in the lattice conductivity below 10 K most of the points exhibited erratic behavior, especially at higher temperatures. This suggests that the estimate of W_i was inadequate. A modification of Eq. (4), which would increase the value of the lattice contribution at higher temperatures, had been suggested previously.[9] This modification consists of adding an additional term to the denominator of Eq. (4), representing the contribution to the electronic thermal resistivity W_e as a result of deviations from Matthiessen's rule. Writing this contribution as ΔW_i, the total electronic thermal resistivity can be given by

$$W_e = W_0 + W_i + \Delta W_i \,. \tag{7}$$

Analogous to the relation between the residual electrical resistivity ρ_0 and the thermal resistivity W_0, it is assumed that

$$\Delta W_i = \Delta\rho_i / LT \,, \tag{8}$$

where $\Delta\rho_i$ are the measured deviations from Matthiessen's rule for electrical resistivity.

The lattice thermal conductivity K_g can then be found from

$$K_g = K - 1/(W_0 + W_i + \Delta W_i) \,, \tag{9}$$

where ΔW_i is given by (8) and increases with temperature, as does $\Delta\rho_i$. This procedure leads to higher values of K_g than does (4).

Uncertainties in the specimen geometry also introduce uncertainties in $\Delta\rho_i$. However, since $\Delta\rho_i$ is typically of the order of 10% of ρ_i or larger, and since the effective specimen geometry could be determined to within 1%, the uncertainty in $\Delta\rho_i$ is, at worst, about 10%.

Following the procedure outlined above, the lattice conductivity K_g for samples 6–8 was redetermined by means of Eq. (9). The results can be seen in Fig. 4 where the three sets of data now follow a more acceptable behavior throughout the entire temperature range.

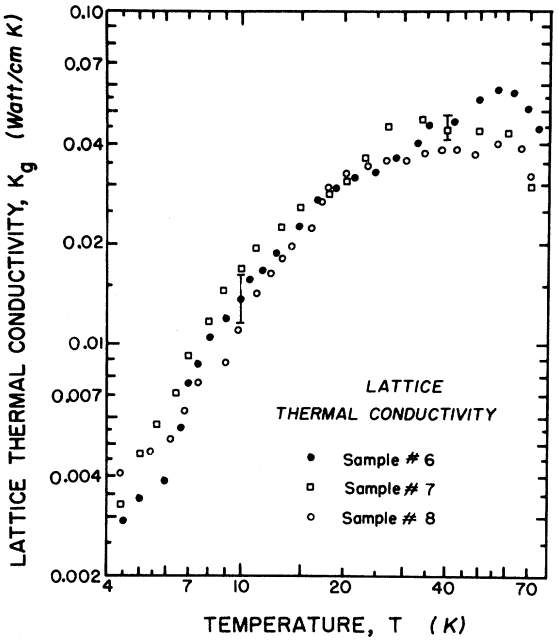

FIG. 4. Lattice thermal conductivity of tin for the same three samples shown in Fig. 3, but derived from Eq. (9).

The probable errors of K_g thus determined are indicated in Fig. 4 at two temperatures. Different quantities entering Eq. (9) have their maximum errors at different temperatures; this fortunate circumstance keeps the over-all error in reasonable bounds over the temperature range shown. At higher temperatures, however, uncertainties in K and in the calculated values of K_e make determinations of K_g increasingly uncertain.

The procedure used depends on the assumption that the deviations from Matthiessen's rule $\Delta\rho_i$ and ΔW_i for electrical and thermal resistivity are related by (8), i.e., by the Wiedemann–Franz law. The relation between these deviations must depend on the mechanism which causes them. Basically, one can ascribe deviations from Matthiessen's rule to three types of causes[10]: (a) changes of the "virtual crystal" with alloying, (b) additional temperature-dependent scattering processes associated with solute atoms, and (c) two or more groups of electrons with different relaxation times contributing to the conductivites (two-band effects).

The first cause can be disregarded for dilute alloys. Deviations due to the second cause obey the Wiedemann–Franz law, as long as the scattering processes are reasonably isotropic in angle. The third type of deviations will generally not obey relation (8), but ΔW_i would be expected to be less than this relation would indicate. This follows because the electrical-conduction relaxation time is more sensitive to the geometry of the Fermi surface.

One would thus expect Eq. (4) to underestimate K_g, and Eq. (9) to overestimate it, with the consequent uncertainty increasing with increasing temperature. However, the fact that (9) led to a reasonable dependence of K_g with temperature may indicate that in the present alloys the deviations from Matthiessen's rule are to a large degree of the second type (additional processes). We shall see below that this conclusion is confirmed by the dependence of $\Delta\rho_i$ on solute content and temperature: The observed dependence is not consistent with the two-band model.

B. Theoretical Interpretation

The lattice thermal conductivity can be expressed in terms of the spectral contribution to the specific heat, an average phonon velocity v, and a relaxation time τ. Using a Debye model for the specific heat and assuming τ to be a function only of the phonon frequency ω (rad/sec), one readily finds

$$K_g = \frac{\hbar^2}{2\pi^2 k T^2 v} \int \frac{e^{\hbar\omega/kT} \tau(\omega) \omega^4 d\omega}{(e^{\hbar\omega/kT} - 1)^2} \quad . \tag{10}$$

The relaxation rate $1/\tau$ is assumed to be additively composed of contributions from various phonon scattering processes. As long as $\tau(\omega)$ does not vary too rapidly with ω, the effect of anharmonic normal processes is small,[6,11] and we shall disregard them. In the present case only three processes need to be considered. These are scattering by the free electrons, scattering by point defects, and anharmonic three-phonon interactions involving the zone boundaries (umklapp processes). The over-all relaxation time $\tau(\omega)$ can thus be given by

$$(1/\tau) = (1/\tau_{pe}) + (1/\tau_d) + (1/\tau_u) \, , \tag{11}$$

where τ_{pe} is the relaxation time of phonons as limited by phonon-electron interactions, τ_d by point defects, and τ_u by umklapp processes. The point defects to be considered are, of course, the solute atoms. Surprisingly enough, the isotopic composition of tin must also be considered.

The relaxation time for point defects τ_d can be expressed in the form[12]

$$\frac{1}{\tau_d} = \frac{3a^3}{G} S^2 \frac{\omega^4}{\pi v^3} = A\omega^4 \, , \tag{12}$$

where a^3 is the volume per atom and $1/G$ is the fractional concentration of defects. The quantity S^2 is a scattering factor that depends on the particular defect involved, and A is defined by Eq. (12). The relaxation time τ_{pe} varies as $1/\omega$; this scattering mechanism dominates at low temperatures where $K_g \propto T^2$. One can thus express[13] τ_{pe} in terms of the measured lattice thermal conductivity, or rather K_g/T^2 at very low tempera-

tures, by

$$\frac{1}{\tau_{pe}} = 7.2\,\frac{2k^3}{\hbar^2 v}\left(\frac{T^2}{K_g}\right)\omega = C\omega\ , \tag{13}$$

where C is defined by the above equation.

The relaxation time for umklapp processes can be written in the form[11]

$$\frac{1}{\tau_u} = 2\gamma^2\,\frac{kT}{Mv^2}\,\frac{\omega^2}{\omega_D}\ , \tag{14}$$

where M is the atomic mass, γ is the Grüneisen constant, and $\omega_D = k\Theta/\hbar$ is the Debye frequency.

One can now express the lattice thermal conductivity, from (10) and (11), in terms of a reduced frequency $x = \hbar\omega/kT$;

$$K_g = \frac{2k^3T^2}{v\hbar^2}\int_0^{\Theta/T}\frac{x^3e^x\,dx}{(e^x-1)^2\,[Ax^3(kT/\hbar)^3 + BT^2x + C]}\ , \tag{15}$$

where, from (14),

$$B = 2\gamma^2 k/(Mv^2\Theta)\ . \tag{16}$$

By adjusting the parameters A, B, and C one can fit theoretical curves derived from (15) to the experimental results.

A suitable Debye temperature Θ_D was obtained by employing data of the specific heat of tin[14] and calculating the variation of Θ_D with temperature from these values.[15] Since most of the lattice conductivity values were taken below 60 K an average value of $\Theta_D = 145$ K was obtained from the specific-heat data.

To obtain a theoretical value of A, the factor S^2/G is to be broken into two parts. One part arises from the distortional strain field around each cadmium atom; the other arises from the fluctuation of the atomic mass of all the atoms about the mean mass. It so happens in the present case that the major contribution to the mass-fluctuation term comes from the isotopes of tin; the cadmium atoms have the same mass as one of the isotopes, and their concentration is low. Thus

$$S^2/G = f_c 3\gamma^2(\Delta R/R)^2 + \tfrac{1}{12}\textstyle\sum_i f_i(\Delta M_i/\bar{M})^2\ . \tag{17}$$

Here f_c is the atomic fraction of cadmium, f_i is the fraction of the various isotopes of tin, γ is again the Grüneisen constant, $\Delta R/R$ is the fractional difference in the radius of solute and solvent atoms, ΔM_i is the difference between the mass of isotopic species and the average mass $\bar{M}$. The distortion term is in the form obtained by Carruthers.[16] (See also Ref 11.) We take $\gamma = 2$, and for $\Delta R/R$ we take -4×10^{-2}, a value obtained from the change in lattice spacings on alloying tin with cadmium.[17] The isotopic abundances were obtained from Ref. 18. The effective value of S^2 thus becomes, for low cadmium concentrations,

$$S^2 = 192\times10^{-4} + 28\times10^{-4}/100f_c\ , \tag{18}$$

where the first term describes scattering due to distortion about the cadmium atoms, and the second term is the isotopic mass effect. In the present case the mass fluctuation contributes about 12% to the total.

The value of v taken to calculate A was 1.75×10^5 cm/sec. The theoretical values of A for samples 6–8 are given in Table II.

The parameter B, describing the strength of the anharmonic interactions, was obtained from Eq. (16) to be $B = 1.8\times10^{-7}\gamma^2\ \mathrm{K}^{-2}$, where we take γ to be an adjustable parameter.

The integral in Eq. (15) was then repeatedly evaluated numerically with A and B being adjusted until a best fit to the experimental data of each sample was obtained. These values of A and B (or actually $2\gamma^2$) were then compared with the theoretical values of A obtained from (12) and (18) and B with $\gamma = 2$. Table II lists the results of this analysis with the experimental values being those that gave the best fit to the data. In all cases the term representing the phonon-electron scattering [Eq. (13)] was taken to be a constant.

The lattice conductivities determined by this fit are shown in Fig. 5, and may be compared to the experimental data of Fig. 4. Also shown in Fig. 5 is the lattice conductivity given by an empirical relation

$$K_g = (1.13\pm0.10)\times10^{-5}\,T^{2.21\pm0.04}/\rho_0^{\,0.21\pm0.04} \tag{19}$$

taken from Gueths *et al.*[3] This dependence was obtained from an analysis of the thermal conductivity in the superconducting state. The broken line in Fig. 5 was obtained from (19) for a residual resistivity of $1\times10^{-6}\ \Omega$ cm, close to that of sample 6. As can be seen, the empirical relation overestimates the lattice thermal conductivity, particularly at higher temperatures, but agrees better below the superconducting temperature, which is the range analyzed in Ref. 3.

In examining Table II we find that the experi-

TABLE II. Experimental and theoretical scattering parameters for lattice thermal conductivity obtained for three samples.[a]

Parameter	Sample No. 6	7	8
A (Theor.)	0.74×10^{-42}	0.86×10^{-42}	0.94×10^{-42}
A (Expt.)	2.57×10^{-42}	2.21×10^{-42}	2.37×10^{-42}
$2\gamma^2$ (Theor.)	8.0	8.0	8.0
$2\gamma^2$ (Expt.)	8.0	12.0	16.0
$(K_g/T^2)^{-1}$	1.8×10^{-4}	2.1×10^{-4}	1.86×10^{-4}

[a]Theoretical values were obtained from the best information available. The experimental data were derived from the best computer fit to the data.

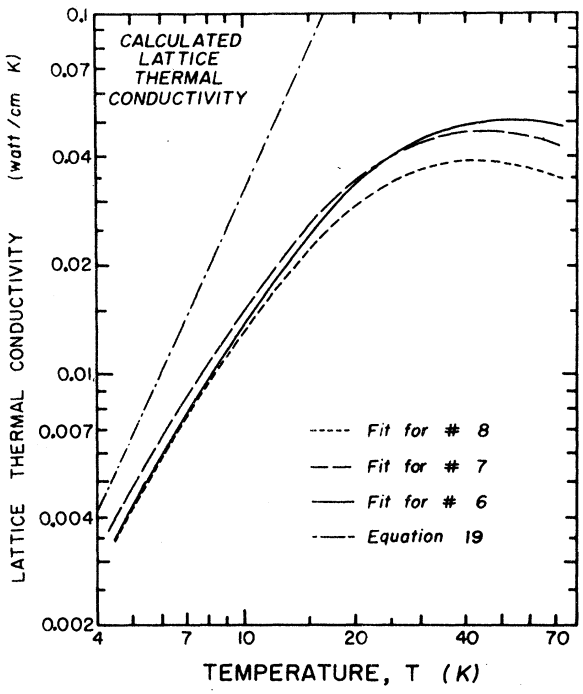

FIG. 5. Values of the lattice thermal conductivity calculated for Eq. (15) using the parameters A, $2\gamma^2$, and $(K_g/T^2)^{-1}$ given in Table II for the three samples. The values determined by Eq. (19) for sample 6 are also shown for comparison.

mental or best fit values used for A and B are always larger than what would be expected from theory. This fact in itself is not unusual, since most of the discrepancies observed by other investigators are also in this same direction.[19–21] Furthermore, when Gueths *et al.*[3] calculated low-temperature lattice conductivity values for the three samples measured here, they used empirical values for the scattering parameter S^2, larger than the theoretical values given by Eq. (18). The discrepancy between theory and experiment in their measurement is similar in magnitude to the discrepancy in ours. It should also be remembered that the value of $\Delta R/R$ used here is a very rough estimate. We have identified $\Delta R/R$ with $\Delta a/a$, the fractional change in the lattice parameter normal to the tetragonal axis. The inclusion of Cd in Sn must also cause electronic changes in the lattice. If these are opposed to the changes due to distortion, one may argue that the true values of $\Delta R/R$ should be larger in magnitude. To fit our measurements as well as those of Gueths *et al.*,[3] one would require that $\Delta R/R$ should be about -7×10^{-2}.

The present measurements give the first determination of the lattice conductivity of tin from single-crystal alloys above the superconducting transition temperature. The lattice conductivity below 12 K, where phonon-electron scattering is the dominant mechanism, follows the T^2 dependence expected from simple theory (e.g., Ref. 13); its magnitude is given approximately by

$$K_g/T^2 = 1.5\times10^{-4}\ \mathrm{W\,cm^{-1}\,K^{-3}}\ . \tag{20}$$

Since the electron-phonon interaction controls not only K_g but also the electronic-conduction properties, one can theoretically relate these quantities. As pointed out elsewhere,[13] it is most advantageous to compare K_g with the ideal thermal resistivity at low temperatures, since the same frequency range of phonons are involved in both, and since the effect of umklapp processes is less pronounced than in the electrical resistivity.

Assuming a spherical Fermi surface, a Debye model for the phonon spectrum, and an electron-phonon interaction of the same strength for all electrons and all polarizations, one obtains the following relation[13]:

$$K_g/T^2 = 313K_i\,T^2/\Theta^4 N_a^{4/3}\ , \tag{21}$$

where K_i is the ideal electronic thermal conductivity at temperature T, Θ is the Debye temperature, and N_a is the number of electrons per atom. Taking the 10 K value of K_i obtained in our previous measurements of pure tin,[1] i.e., $K_iT^2 = 1\times10^3$ $\mathrm{W\,cm^{-1}\,K}$, taking $\Theta = 145$ K as above, and taking $N_a = 4$, we obtain a theoretically expected value of

$$K_g/T^2 = 1.2\times10^{-4}\ \mathrm{W\,cm^{-1}\,K^{-3}}\ , \tag{22}$$

which may be compared with the experimental value of Eq. (20).

Before one rejoices at this good agreement, the following facts should be considered:

(a) The agreement is very sensitive to the choice of Θ; with $\Theta = 165$ K, for example, the theoretical value of K_g would be reduced by a factor of almost 1.7, leading to a discrepancy of a factor of 2.

(b) The model of a spherical Fermi surface, where all parts of the Fermi surface contribute equally both to the electronic conduction and to phonon scattering, is too simple, and not in accord with the model used to explain the anisotropic conductivities of tin.[1] According to that model only a fraction of the spherical Fermi surface contributes to the conductivity. If only half the Fermi surface contributes to electronic conduction, but the phonon-electron scattering is the same on all parts of the Fermi surface, the ratio K_g/K_i should be increased by a factor of 2. If parts of the nonconducting Fermi sphere are eliminated because of contact with zone boundaries, this ratio would be further increased. If, on the other hand, the electron-phonon interaction is stronger on the nonconducting segments of the Fermi surface, as it well may be because the proximity of zone boundaries makes the electrons less free, the ratio K_g/K_i would be reduced again. The agreement with (21)

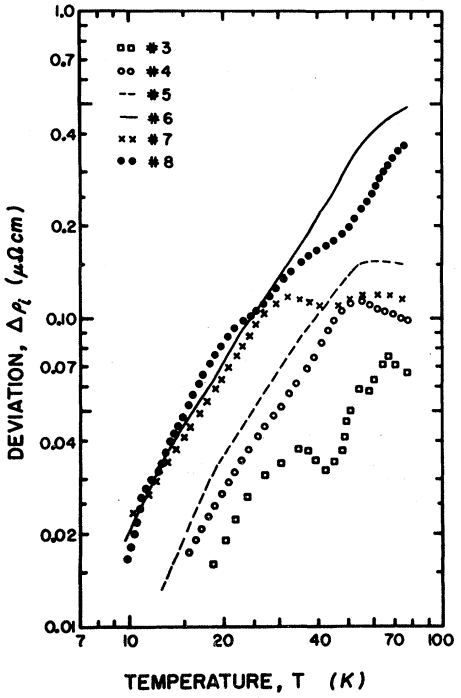

FIG. 6. Measured deviations from Matthiessen's rule for all six alloy samples.

may thus be a fortuitous cancellation of the above factors.

(c) Finally, it should be remembered that K_i in tin departs strongly from a T^{-2} dependence,[1] and that the specific heat varies faster than T^3 in that temperature range. We had previously invoked the anomalous temperature dependence of the specific heat to account for the temperature dependence of K_i. One may, of course, argue that the effects of dispersion will be less pronounced in K_g than in the specific heat, because the integral (15) gives less weight to the higher frequencies. However, it is clear that a more detailed theoretical treatment is required.

V. DEVIATIONS FROM MATTHIESSEN'S RULE

Deviations from Matthiessen's rule, as defined by Eq. (2), have been determined from the measured electrical resistivities of the six alloy samples, from their residual resistivities, taken to be their resistivities at 4.2 K, and from the ideal electrical resistivity $\rho_i(T)$ of tin in the same orientation. The latter was deduced from previous measurements[1] of the ideal electrical resistivities of two single crystals of tin. These deviations are displayed in Fig. 6 as functions of temperature.

The deviations generally increase with increasing solute content and with temperature, except for sample 3. All the deviations are substantially larger than ρ_i at the same temperature, but are, of course, only a small fraction of the total resistivity. Except for sample 3, all deviations vary roughly as T^2 below 40 K.

The deviations from Matthiessen's rule are not only of intrinsic interest, but are related to corresponding deviations from additivity of the electronic thermal resistivity [Eq. (7)] discussed above. In principle, one can attribute deviations to three causes[10] (as pointed out above): (a) changes in the band structure and the phonon spectrum due to alloying; (b) additional temperature-dependent scattering processes associated with solute atoms, in particular, phonon-assisted impurity scattering processes, where electrons are scattered by solute atoms with the emission or absorption of phonons. To first order these processes arise either from the phonon-induced displacement of the impurity potential (Koshino effect[22]) or from the distortion of the impurity potential by the strain of a phonon[23]; and (c) deviations which arise because two or more groups of electrons contribute to the conductivity. The reciprocal of each partial conductivity is composed of an ideal and a residual resistivity. If these two resistivities scale differently for each group, the over-all resistivity shows a deviation. This is typified by the two-band effect of Sondheimer and Wilson.[24]

It can reasonably be assumed that any deviations in Matthiessen's rule caused by changes in the phonon spectrum or the band structure due to alloying would be smaller than the observed deviations. We are dealing with dilute alloys of less than 1-at.% solute content. The fractional change in electron concentration is comparable, and the change in elastic properties is quite small. We would expect $\Delta\rho_i/\rho_i$ due to this cause to be of the order of 1%. The observed deviations are much larger. Thus we shall only consider either the two-band model or phonon-assisted impurity scattering.

The two-band model is attractive because we believe, from the anisotropies of the electrical and thermal conductivities, that there are two regions which contribute mainly to the conductivities, one about the tetragonal axis, and a series of equivalent regions perpendicular to it. At low temperatures the former has a relatively higher ideal electrical resistivity, and this is reflected in an electrical resistivity anisotropy which is temperature dependent and rises rapidly below 40 K.[1] However, while the detailed expressions for the deviations are complicated and contain parameters which are not easily derived from first principles, the present deviations are in conflict with the following limiting results which the two-band model predicts: At low temperatures, where $\rho_0 \gg \rho_i$, $\Delta\rho_i$ should be independent of ρ_0 and proportional to $\rho_i(T)$, while at higher temperatures, where $\rho_i \gg \rho_0$, $\Delta\rho_i$ should

be independent of T and proportional to ρ_0. The residual resistivity is too high for the second limit to apply to the present measurements, but the first limit is clearly appropriate over most of the temperature range; yet the measured values of $\Delta\rho_i$ are clearly not independent of ρ_0 but increase roughly proportionally to ρ_0.

Very roughly, one can fit the measured deviations to an expression of the form

$$\Delta\rho_i = b\rho_0 T^2 , \tag{23}$$

where ρ_0 is the residual resistivity and b is a parameter.

A computer fit of the measured deviations shown in Fig. 6 was then made to the above relation with an optimum constant being determined for each sample. The values obtained are listed in Table I for all six alloy samples. With the exception of the odd sample No. 6, the constant b had an average value of $5.2\times10^{-5}\ \mathrm{K}^{-2}$.

The dependence on ρ_0 suggests that the deviations arise from phonon-assisted impurity scattering. Our data are not sufficiently extensive, nor is the fit to (23) so good, that one can rule out contributions from the two-band effect or decide its relative importance. The fact that the major contribution to $\Delta\rho_i$ comes from phonon-assisted impurity scattering lends support to the procedure used to calculate K_e and to deduce K_g.

In the limit of low temperatures, when $\rho_i \propto T^5$, $\Delta\rho_i \propto T^4$ if the additional scattering arises from the distortion of the impurity potential,[23] and $\Delta\rho_i \propto T^2$ if it arises from the displacement (Koshino effect[22]). The observed $\Delta\rho_i$ varies as T^2; this would favor the Koshino effect, except that the observations of $\Delta\rho_i$ do not extend to really low temperatures, as evidenced by the fact that in the same temperature range (15–40 K), ρ_i varies as $T^{2.5}$. It is thus not clear to what extent the phonon-assisted impurity scattering should be ascribed to the strain model[23] and to the Koshino effect.[22]

One difficulty with the Koshino effect, where the additional scattering arises from the displacement of the impurity potential, is that one can show that this effect vanishes for a free-electron gas.[25] On the other hand, if the wave function of the conduction electrons is heavily modulated, some effect remains, and has to be considered together with the distortion effect.[10] Normally, one thinks of the conduction electrons in tin to behave like free electrons, so that the Koshino effect should be small. Clearly the deviations from Matthiessen's rule in tin alloys merit further theoretical and experimental study.

ACKNOWLEDGMENTS

Three of us (M. C. K., P. G. K., and F. P. L.) acknowledge the guidance and leadership provided by Professor C. A. Reynolds, who died soon after this work was completed. The authors wish to thank H. Taylor for providing cryogenic liquids, and Miss L. C. Harrington, Dr. T. K. Chu, D. Strom, and M. Simard for technical assistance.

---

*Presented as partial requirement for the Ph. D. degree of Michael C. Karamargin, whose work was performed under the Long Term Education and Training Program of the U. S. Navy. The work was also partially supported by the U. S. Army Research Office, Durham and the University of Connecticut Research Foundation. Helium used was supplied by the Office of Naval Research.

†Present address: Naval Underwater Systems Center, New London Laboratory, New London, Conn. 06320.

‡Deceased.

[1]M. C. Karamargin, C. A. Reynolds, F. P. Lipschultz, and P. G. Klemens, Phys. Rev. B 5, 2856 (1972).

[2]P. W. Bridgeman, Proc. Am. Acad. Arts Sci. 60, 305 (1925).

[3]J. E. Gueths, P. L. Garbarino, M. A. Mitchell, P. G. Klemens, and C. A. Reynolds, Phys. Rev. 178, 1009 (1969).

[4]J. E. Gueths, F. V. Burckbuchler, and C. A. Reynolds, Rev. Sci. Instr. 40, 1344 (1969).

[5]J. E. Gueths, C. A. Reynolds, and M. A. Mitchell, Phys. Rev. 150, 346 (1966).

[6]P. G. Klemens, Solid State Phys. 7, 1 (1958).

[7]W. R. G. Kemp, P. G. Klemens, A. K. Sreedhar, and G. K. White, Phil. Mag. 46, 811 (1955).

[8]W. R. G. Kemp, P. G. Klemens, A. K. Sreedhar, and G. K. White, Proc. Roy. Soc. (London) A223, 480 (1956).

[9]P. G. Klemens, Australian J. Phys. 12, 199 (1959).

[10]D. H. Damon, M. P. Mathur, and P. G. Klemens, Phys. Rev. 176, 876 (1968).

[11]P. G. Klemens, in *Thermal Conductivity*, edited by R. P. Tye (Academic, New York, 1969), Vol. 1, p. 1.

[12]P. G. Klemens, Proc. Phys. Soc. (London) A68, 1113 (1955).

[13]P. G. Klemens, in *Handbuch der Physik* edited by S. Flügge (Springer, Berlin, 1956), Vol. 14, p. 198.

[14]R. J. Corruccini and J. J. Gniewek, Natl. Bur. Stds. Monograph 21 (U.S. GPO, Washington, D. C., 1960).

[15]G. T. Furakawa, W. G. Saba, and M. L. Reilly, NSRDS-NBS 18 (U.S. GPO, Washington, D. C., 1968).

[16]P. Carruthers, Rev. Mod. Phys. 33, 92 (1961).

[17]J. A. Lee and G. V. Raynor, Proc. Phys. Soc. (London) B67, 737 (1954).

[18]R. B. Leighton, *Principles of Modern Physics* (McGraw-Hill, New York, 1959).

[19]P. G. Klemens, G. K. White, and R. J. Tainsh, Phil. Mag. 7, 1323 (1962).

[20]J. J. Martin and G. C. Danielson, Phys. Rev. 166, 879 (1968).

[21]G. van Baarle and R. P. Huebener, Phys. Rev. 172, 699 (1968).

[22]P. G. Koshino, Progr. Theoret. Phys. (Kyoto) 24, 484 (1960); 24, 1049 (1960).

[23]P. G. Klemens, J. Phys. Soc. Japan Suppl. 18, II77

(1963).
[24]E. H. Sondheimer and A. H. Wilson, Proc. Roy. Soc. (London) A203, 75 (1950).
[25]P. L. Taylor, Proc. Phys. Soc. (London) A80, 755 (1962); Phys. Rev. 135, A1333 (1964).

PHYSICAL REVIEW B VOLUME 6, NUMBER 10 15 NOVEMBER 1972

Pseudopotential Calculations of the Electronic Structure of a Transition-Metal Compound—Niobium Nitride

C. Y. Fong
Department of Physics, University of California, Davis, California 95616

and

Marvin L. Cohen*
Department of Physics, University of California, and Inorganic Material Research Division, Lawrence Berkeley Laboratory, Berkeley, California 94720

(Received 2 May 1972)

The electronic band structure, density of states, and $\epsilon_2(\omega)$, the imaginary part of the dielectric constant, are calculated for niobium nitride using the empirical-pseudopotential method. The results are compared with non-self-consistent and with the self-consistent augmented-plane-wave calculations. A discussion of the Fermi surface is included.

I. INTRODUCTION

We have recently developed a scheme,[1] which is a simple modification of the usual form of the empirical-pseudopotential method[2] (EPM) for simple metals and semiconductors, to calculate the electronic properties of noble metals[3] and a transition metal—niobium.[4] The advantage of this scheme is its simplicity and its flexibility. In the case of the noble metals and the transition metal, this empirical scheme involves less (8) parameters than previous pseudopotential–tight-binding schemes. It is also unnecessary to know *a priori* the region in the Brillouin zone (BZ) where the hybridization between the *s* and *d* electrons is strongest for these crystals. All one needs are the energies at a few high-symmetry points inside the BZ and the width of the *d* bands. The energies and the width of the *d* bands can be determined by optical measurements[3,5] and photoemission experiments,[6] respectively. Furthermore, the atomic pseudopotential extracted from one calculation can be used at least as a starting potential for other compounds with the same atom as a constituent.[2] It is this flexibility which enables us to calculate the electronic properties of a series of compounds.

In this report we concentrate on a transition-metal compound. This class of compounds is extremely interesting. Some of these compounds are high-temperature superconductors, and others exhibit interesting metal-insulator transitions. It is felt that a vast amount of basic knowledge about solids can be obtained through studies of these kinds of crystals, and it is, therefore, necessary to have an effective method to study the electronic properties of these compounds. We have anticipated in Ref. 1 that the EPM can be used for this purpose. Here, we report the first energy band structure of a transition-metal compound (niobium nitrade) obtained by using the EPM. We would like to make a few comments about the significance of the present calculation: (a) Despite the fact that the band structure presented is fitted to first-principles calculations (due to the lack of experimental information) the results indicate that it is now possible to determine with even more accuracy the energy band structure of interesting transition-metal compounds if optical and photoemission data are available. (b) NbN is a high-temperature superconductor with $T = 15.7\,^{\circ}\mathrm{K}$.[7] We anticipate that the pseudopotential derived here for NbN can be used in the future to study the origin of the high superconducting transition temperature for this compound. Furthermore, if more optical and photoemission data relating to the transition-metal compounds are available, one can use the results of the EPM to predict the superconducting transition temperature. (c) Experimental studies on NbN, up to present, are restricted to mechanical, electrical, and superconducting properties. If optical data were available we could refine our calculation. For the present, we give a calculation of the imaginary part of the dielectric function as a rough prediction of the optical spectrum. (d) Earlier theoretical studies were done by Mattheiss[8] (who also summarized results for similar compounds) using